Atmospheric carbon dioxide variations at Mauna Loa Observatory, Hawaii

By CHARLES D. KEELING, ROBERT B. BACASTOW, ARNOLD E. BAINBRIDGE, CARL A. EKDAHL, JR, PETER R. GUENTHER, and LEE S. WATERMAN, *Scripps Institution of Oceanography, University of California at San Diego, La Jolla, California, USA* and JOHN F. S. CHIN, *National Oceanic and Atmospheric Administration, Mauna Loa Observatory, Hawaii*

(Manuscript received February 16, 1973; in final form January 27, 1976)

John Noble
Earth 206, UCSC
March 2009
(Updated)

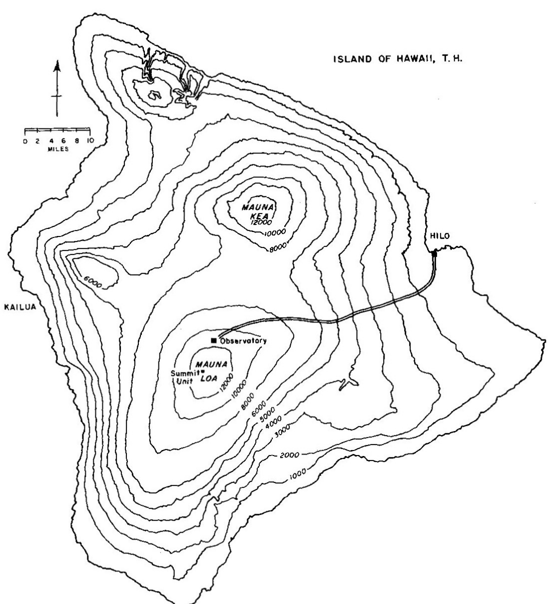

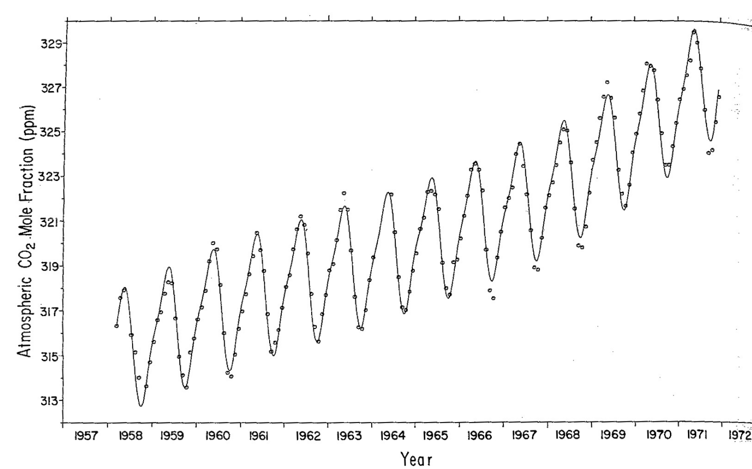

Charles Keeling

- Ph.D. in polymer chemistry from Univ. of Illinois
  - He liked the west, outdoors, hiking in the cascades…
- Post-doc at Cal Tech
  - First studied uranium in rocks
  - Then studied CO_2 in river water; he couldn't understand CO_2 amounts in rivers until he understood it in the air
  - His primary motivation was that it was fun to go out on camping trips in nature.

Mauna Loa Observatory

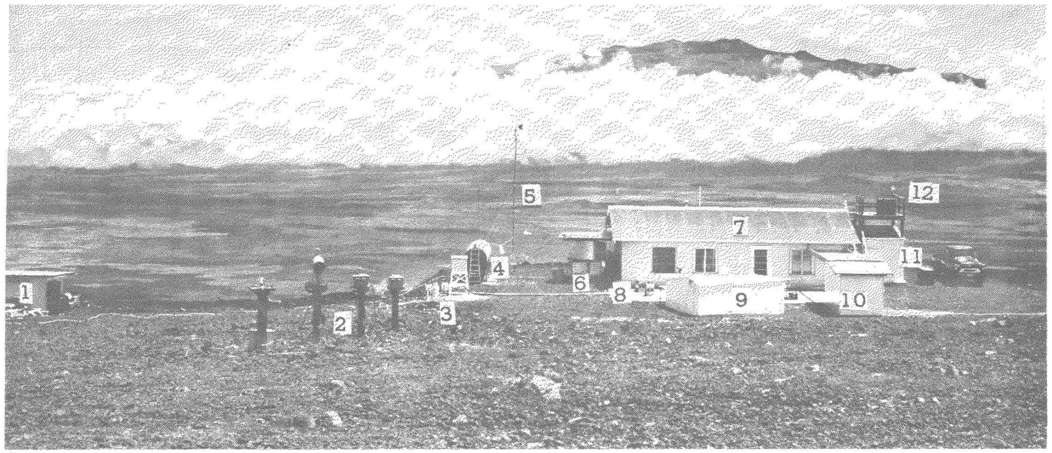

FIGURE 6.—The Mauna Loa Observatory, looking north. From left to right: (1) generator shed, (2) solar radiation instruments, (3) rain gages and instrument shelter, (4) diesel fuel tank, (5) anemometer mast, (6) water tank, (7) main building, (8) concrete apron, (9) Kiess-Corliss spectrograph shelter (see reference [6]), (10) *Dobson spectrophotometer housing*, (11) instrument platform, (12) fission products collector. In the background is Mauna Kea, about 25 miles distant. Intervening clouds are trade wind cumuli and lie over the saddle and below the level of the Observatory.

(Price and Pales 1959)

Detectable local CO_2 sources:

- upslope volcano
- vegetation 30 km east
- diesel generator (until July 1967)
- daytime automobile pollution

(Pales and Keeling 1965)

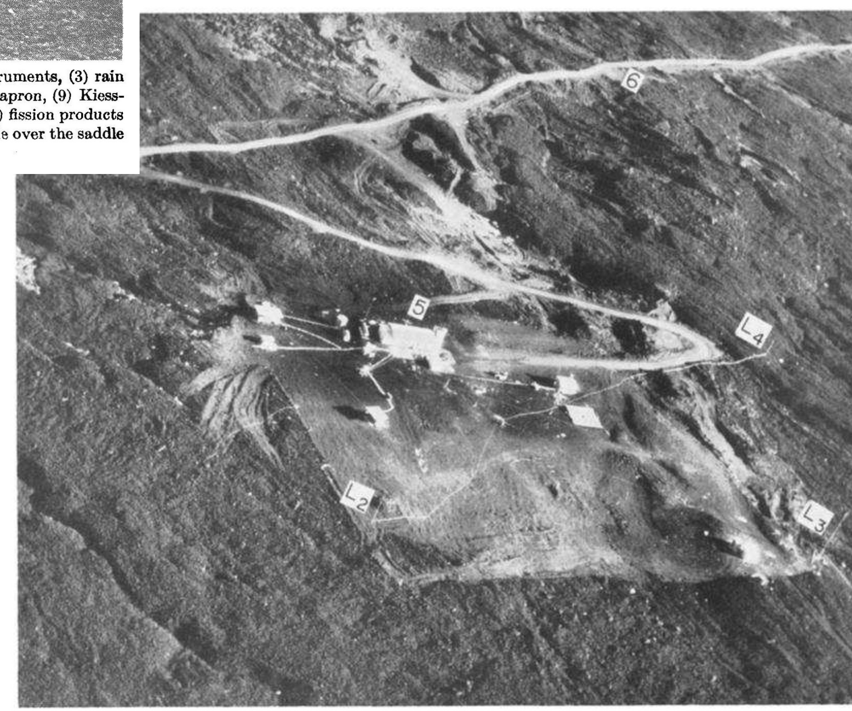

Fig. 2. Aerial view of the observatory, looking north (downslope). L_1 to L_4 are air intake towers. (5) is the main observatory building which houses the analyzer. Aluminum tubing between the towers and the observatory is partially visible. (6) is the road to Hilo. Photograph was taken in August 1962.

Observatory is located on lava flow on north slope of largest active volcano.

Volcanic emanations of CO_2 near the summit of Mauna Loa and uptake of CO_2 on the forested lower slopes of the mountain influence the concentration of CO_2 at Mauna Loa Observatory, but do not seriously interfere with the determination of regional changes. (Pales and Keeling 1965)

Mauna Loa Observatory

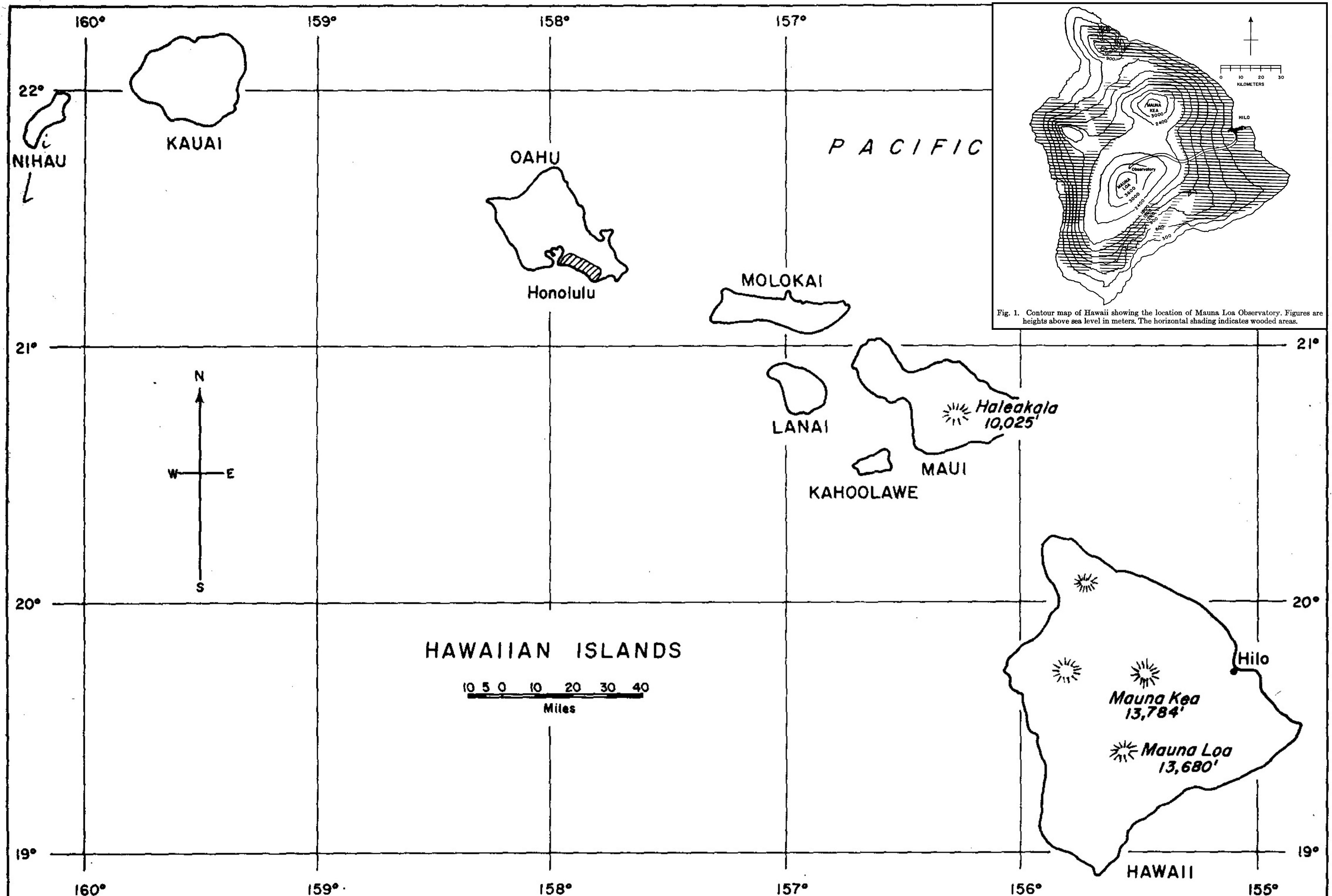

Fig. 1. Contour map of Hawaii showing the location of Mauna Loa Observatory. Figures are heights above sea level in meters. The horizontal shading indicates wooded areas.

Local meteorology

TABLE 1.—*Temperature (° F.) at or near Mauna Loa Observatory*

	Jan.	Feb.	Mar.	Apr.	May	June	July	Aug.	Sept.	Oct.	Nov.	Dec.
Highest of record	62	63	60	65	68	70	70	69	67	68	64	67
Mean maximum	48. 4	46. 6	49. 3	53. 6	55. 8	58. 8	56. 7	56. 6	57. 8	56. 5	53. 0	49. 6
Mean minimum	29. 6	28. 9	31. 3	33. 7	34. 5	37. 1	35. 6	36. 6	36. 7	36. 6	33. 3	31. 9
Lowest of record	22	20	20	25	24	24	26	29	29	29	23	22
Mean daily range	18. 8	17. 7	18. 0	19. 9	21. 3	21. 7	21. 1	20. 0	21. 1	19. 9	19. 7	17. 7
Years of record	6	5	4	6	6	6	6	5	5	5	5	5

TABLE 3.—*Mean hourly winds at Mauna Loa Observatory*

January 1958, Monthly Mean 9.1 m.p.h.

Hour ending (LST)	01	02	03	04	05	06	07*	08	09	10	11	12	13	14	15	16	17	18*	19	20	21	22	23	24
Percentage W through E	19	13	16	13	16	16	16	16	19	71	90	100	100	100	100	100	94	74	61	42	19	16	13	16
Percentage SE through SW	81	87	84	87	84	84	84	84	77	26	10	0	0	0	0	0	6	23	29	58	81	84	87	84
Mean wind speed (m.p.h.)	9. 4	9. 4	9. 6	9. 8	10. 7	10. 3	9. 9	9. 8	7. 0	5. 5	7. 1	7. 6	9. 5	10. 1	10. 2	9. 6	8. 9	7. 6	6. 9	8. 2	9. 2	9. 5	10. 2	10. 6

July 1958, Monthly Mean 9.5 m.p.h.

Hour ending (LST)	01	02	03	04	05	06	07	08	09	10	11	12	13	14	15	16	17	18	19*	20	21	22	23	24
Percentage W through E	0	0	0	0	0	0	0	39	81	84	94	90	90	97	97	97	100	94	90	48	10	6	6	3
Percentage SE through SW	97	97	97	100	94	100	100	52	19	16	6	10	3	3	3	3	0	6	6	45	81	94	90	97
Mean wind speed (m.p.h.)	11. 5	10. 6	10. 8	10. 3	10. 5	10. 1	9. 4	7. 1	7. 3	8. 3	9. 4	10. 5	11. 0	10. 8	10. 6	9. 9	9. 4	8. 5	7. 7	6. 4	7. 3	9. 3	10. 2	10. 5

*Indicates sunrise and sunset.
Underscore indicates minimum wind speed.
Double underscore indicates maximum wind speed.

TABLE 2.—*Precipitation at Mauna Loa Observatory*

A. Mean Monthly Rainfall		B. Hourly Rainfall, Percentage Frequency (trace or more) of All Observations			
Month	Inches	Hour ending (LST)	%	Hour ending (LST)	%
January	3. 9	01	2. 0	13	4. 9
February	2. 1	02	2. 6	14	6. 6
March	4. 0	03	2. 0	15	6. 1
April	0. 7	04	2. 0	16	6. 4
May	1. 2	05	2. 3	17	7. 5
June	0. 3	06	2. 6	18	6. 4
July	2. 0	07	2. 6	19	4. 0
August	2. 9	08	2. 9	20	4. 0
September	1. 9	09	2. 3	21	2. 6
October	1. 2	10	3. 2	22	1. 7
November	1. 5	11	3. 5	23	1. 7
December	3. 4	12	4. 0	24	2. 3

(Price and Pales 1959)

Hygrothermograph chart

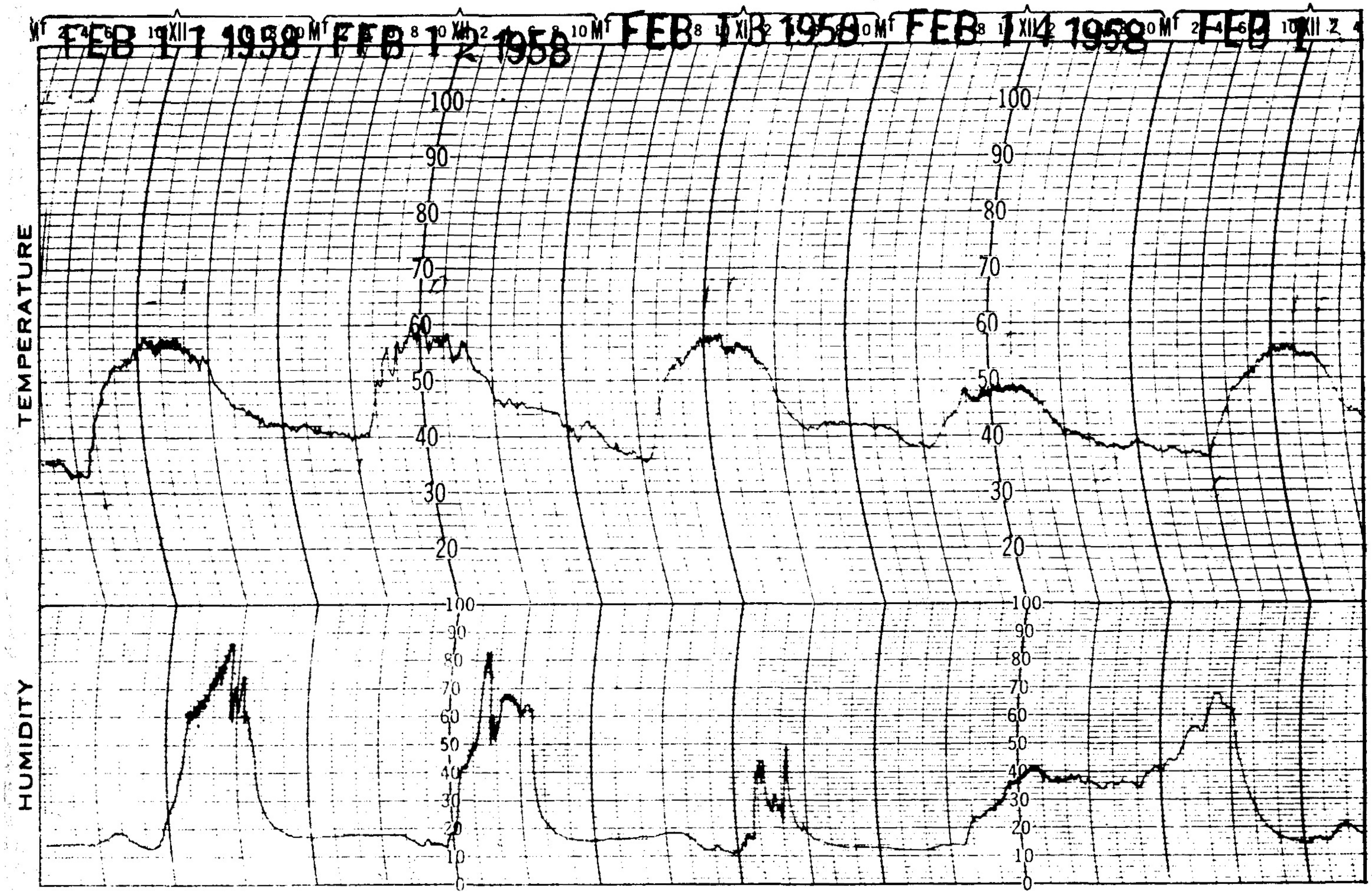

FIGURE 8.—A representative hygrothermograph chart, Mauna Loa Observatory. The tendency for humidity to increase during the afternoon probably reflects the influx of air from lower levels.

A representative hygrothermograph chart, Mauna Loa Observatory. The tendency for humidity to increase during the afternoon probably reflects the influx of air from lower levels.

(Price and Pales 1959)

Instrumentation: infrared analyzer

Applied Physics Corporation* dual detector infrared analyzer

- Measures CO_2 mixing ratio
- $\sigma \approx 0.3$ ppm for individual comparison
- $\sigma \approx 0.5$ ppm for two reference gases

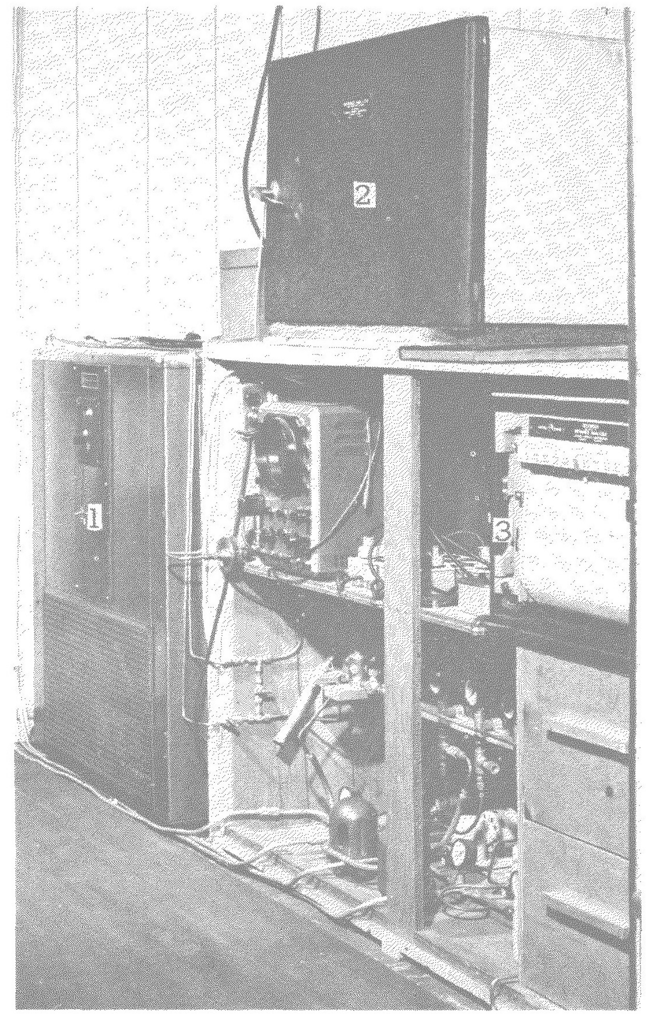

FIGURE 11.—Infrared analyzer for CO_2. (1) freezer to remove water vapor which would otherwise interfere with the analysis, (2) analyzer box, (3) recorder.

* APP→ Cary Instruments (division of Varian) in 1966

(Price and Pales 1959)

Adjusted CO_2 index

- A mole fraction scale proportional to instrument response, informally known as Scripps index. Est. 1957

- Linear relation between index and mole fraction of CO_2 was determined in the 310–330 ppm range, “where linearity in instrument response could be reasonably assumed”.

Infrared analyzer

- Measures energy loss of IR beam traversing a gas sample.
- Radiation emitted by a glowing nichrome filament is mechanically chopped at 20 c.p.s. and then directed through the gas sample into a detector cell which is permanently filled with CO_2 diluted with argon.
- Radiation absorbed by CO_2 gas produces a cyclic pulsation in pressure that is transmitted to a tantalum diaphragm of a condenser microphone and then converted to an alternating voltage, amplified, and recorded.
- The presence of CO_2 in the gas sample stream reduces the radiation reaching the detector cell at just those wavelengths at which absorption can occur in the detector.
- Thus the voltage developed by the detector varies inversely with the CO_2 concentration in the gas sample. This voltage is plotted by a strip chart recorder which thereby furnishes a continuous record of the concentration of CO_2 in the gas sample stream.

Air flow system for atmospheric CO_2

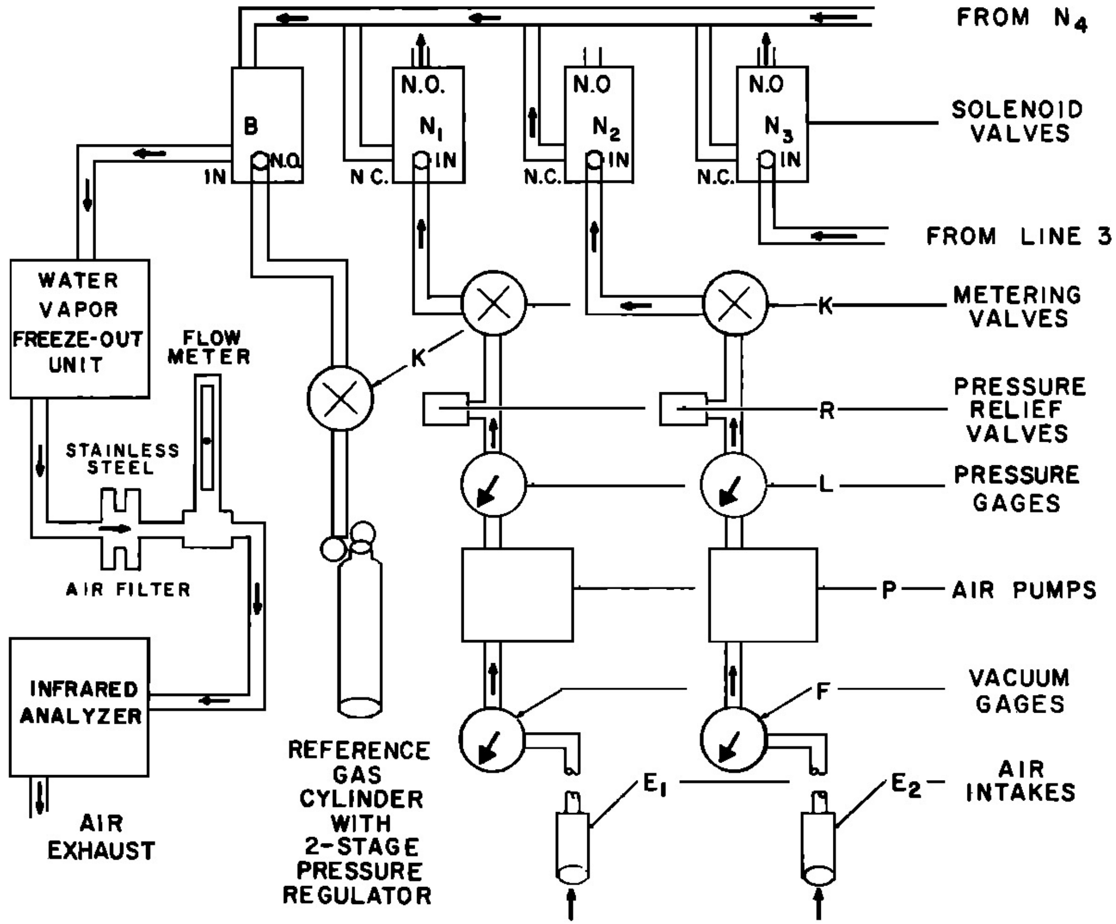

Fig. 3. Air flow system for atmospheric CO_2. Letters are explained in the text. N.O., normally open; N.C., normally closed.

(Pales & Keeling 1965)

Concentration of atmospheric CO_2, 1958–1972

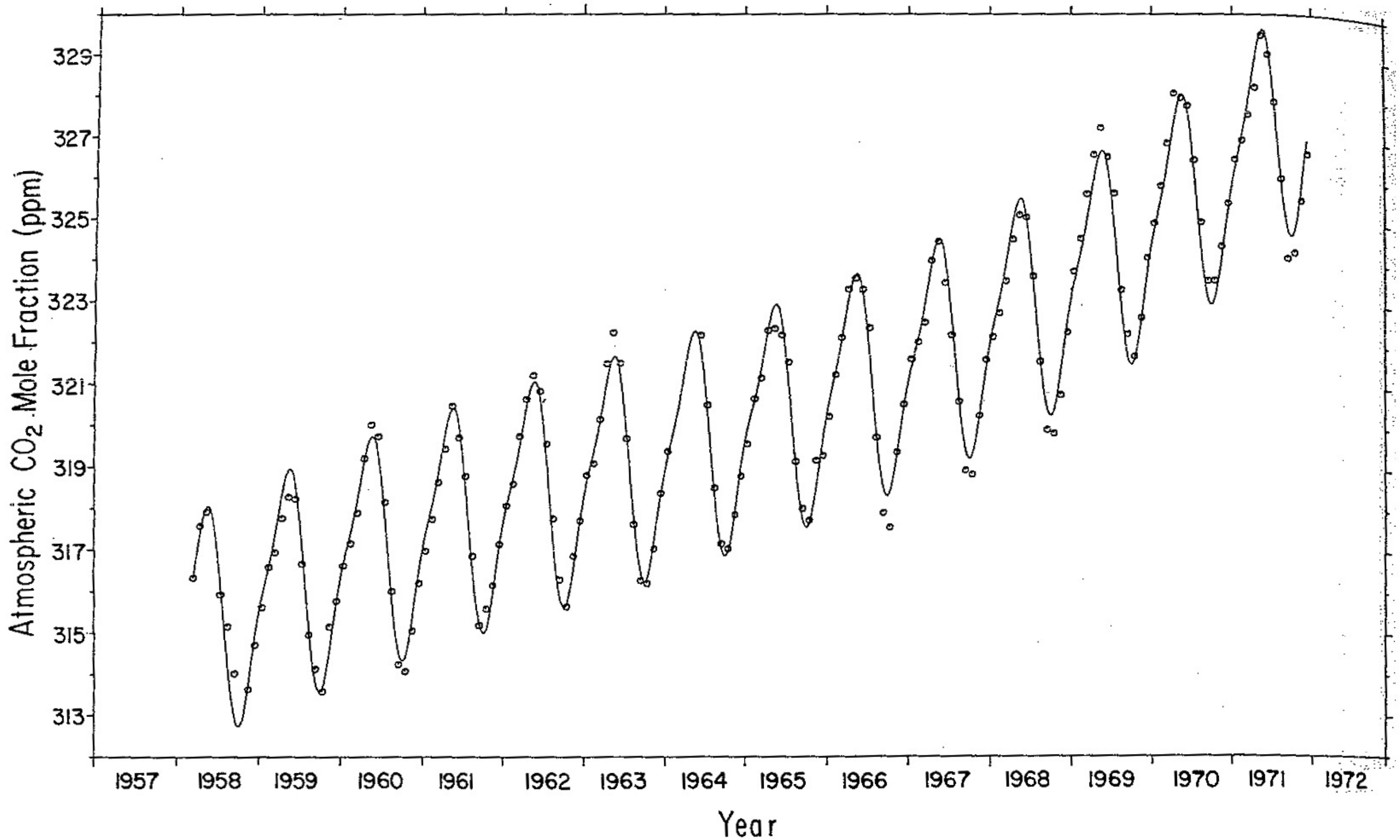

Fig. 5. Long term variation in the concentration of atmospheric CO_2 at Mauna Loa Observatory. The circles indicate the observed monthly average concentration. The oscillatory curve is a least squares fit to these averages of an empirical equation containing 6 and 12 month cyclic terms and a cubic trend function, chosen to contain powers of time up to the third. Concentrations are plotted as the CO_2 mole fraction of dry air in ppm.

(Keeling *et al.* 1976)

Manometric calibration methods

1. Analysis in which CO_2 is separated from carrier gas using liquid nitrogen freeze-out technology.

2. Synthesis in which CO_2 is mixed with carrier gases in accurately determined proportions and compared with reference gases by IR analysis.
   - carrier gases: N, O_2, Ar

Carrier gases

Table 1. *Apparent downward shift in CO_2 mole fraction (in ppm) as measured by applied Physics Model 70 Infrared Analyzer when nitrogen is substituted for carrier gas as specified*

Method	Adjusted CO_2 index	Carrier gas: 79.1 % N_2, 20.9 % O_2	Carrier gas: 99.07 % N_2, 0.93 % A	Carrier gas: CO_2-free air
Analysis	310	3.50	.20[a]	3.70
Synthesis		3.44	.24	3.68[b]
Analysis	320	3.68	.21[a]	3.89
Synthesis		3.63	.25	3.88[b]
Analysis	330	3.87	.23[a]	4.10
Synthesis		3.82	.26	4.08[b]

[a] Determined by difference.
[b] Determined by sum.

(Keeling *et al.* 1976)

Hourly average CO_2 concentration

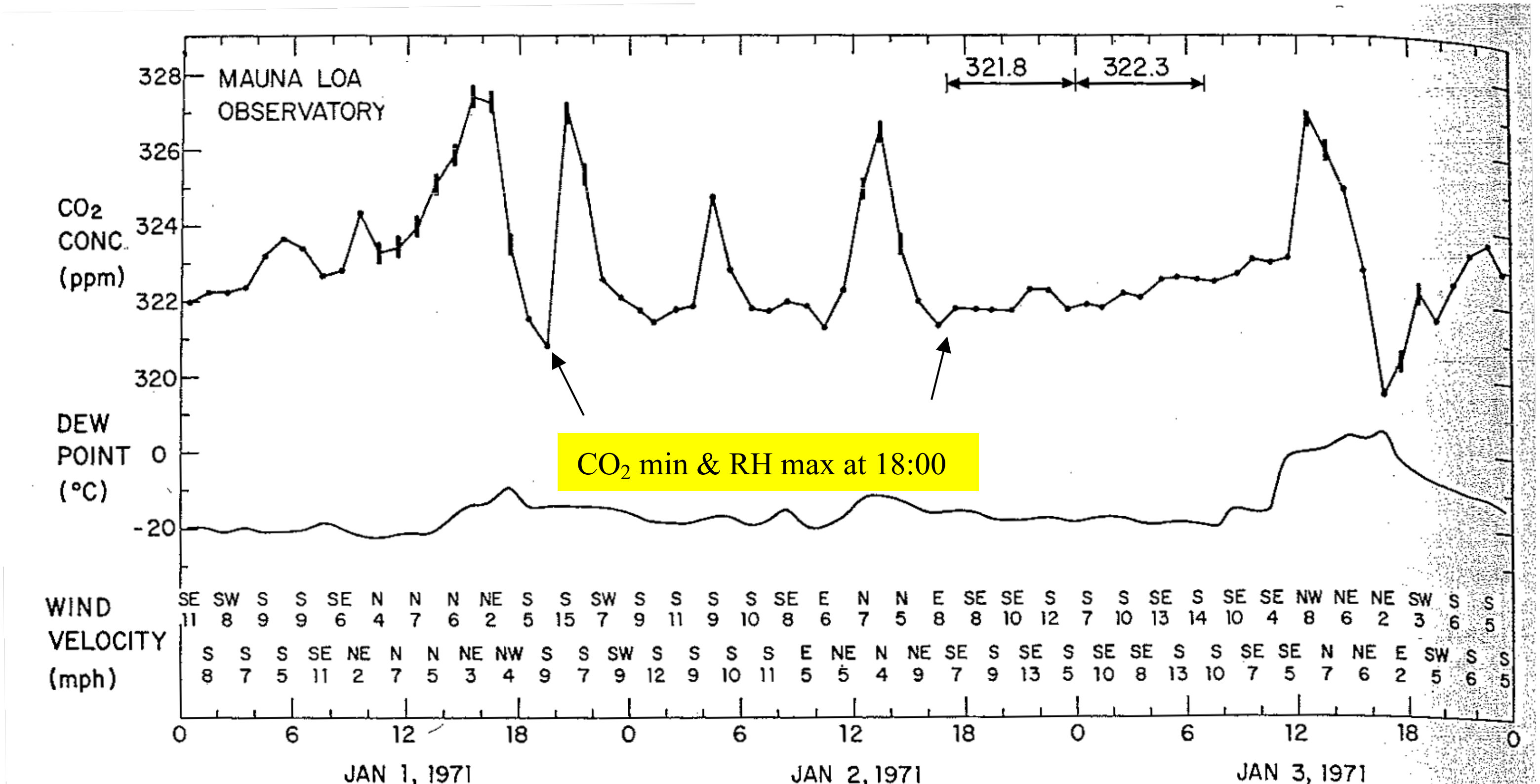

Fig. 1. Hourly average atmospheric CO_2 concentration at Mauna Loa Observatory versus time during the first three days of 1971. Concentrations are plotted on the adjusted CO_2 index scale. Vertical bars indicate periods during which the record trace was variable, indicating local contamination. Horizontal arrows indicate periods of steady concentration. The average concentration for each steady period is indicated above the arrow.

Persistent diurnal variation

- 0:00 → low-humidity air blows downslope
- Am: upslope wind develops and brings sub-inversion layer air

(Keeling *et al.* 1976)

Uncertainties

- Inaccuracy of manometric standard gases
- Imprecision in IR comparisons
- No procedure can prove the absence of undetected systematic errors

Mauna Loa data features

- Seasonal oscillation
- Long-term increase
- Meteorological conditions
  - Air is above trade wind layer
  - Local contamination

Seasonal oscillation

- Reflects integrated uptake & release of CO_2 by land plants & soil

- Amplitude:
  - Maximum in Arctic; NH > SH
    - due to NH boreal vs. austral predominance
  - Decreases with decreasing latitude towards SH mid-latitudes
  - Decreases with height above the ground
    - due to mixing
  - Varies seasonally: 6 ppm annual average
  - 0.7 ppm ↑ yr^{-1} (Pales and Keeling 1965)

- Data reflects changes in air above trade winds, essentially the same as aloft except in summer

CO_2 long-term increase

- CO_2 concentration annual increase ≈ 1 ppm dry air
  - Represents ~ half of combustion contribution.
- CO_2 rate of increase is not proportional to fossil fuel combustion rate in either hemisphere.

800,000-year CO_2 & temperature record

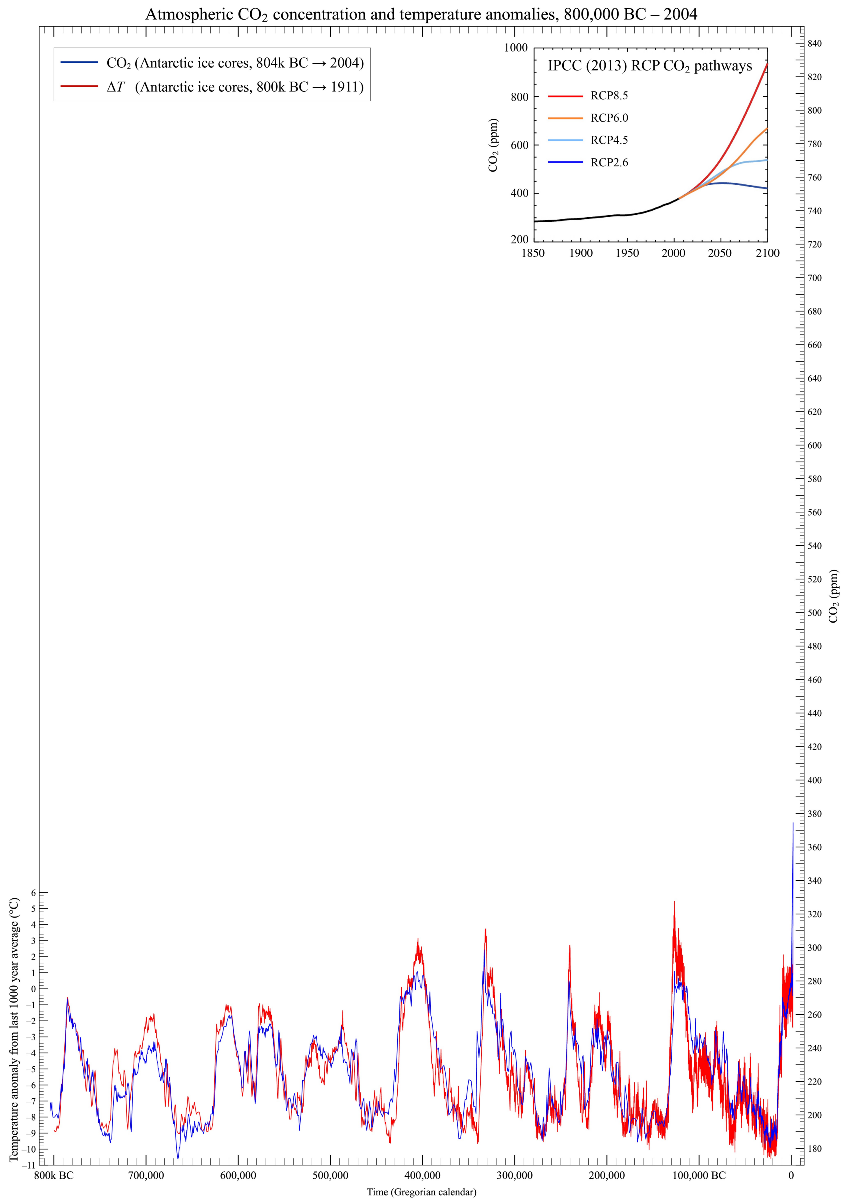

(Noble 2024)

800,000-year CO_2 & temperature record

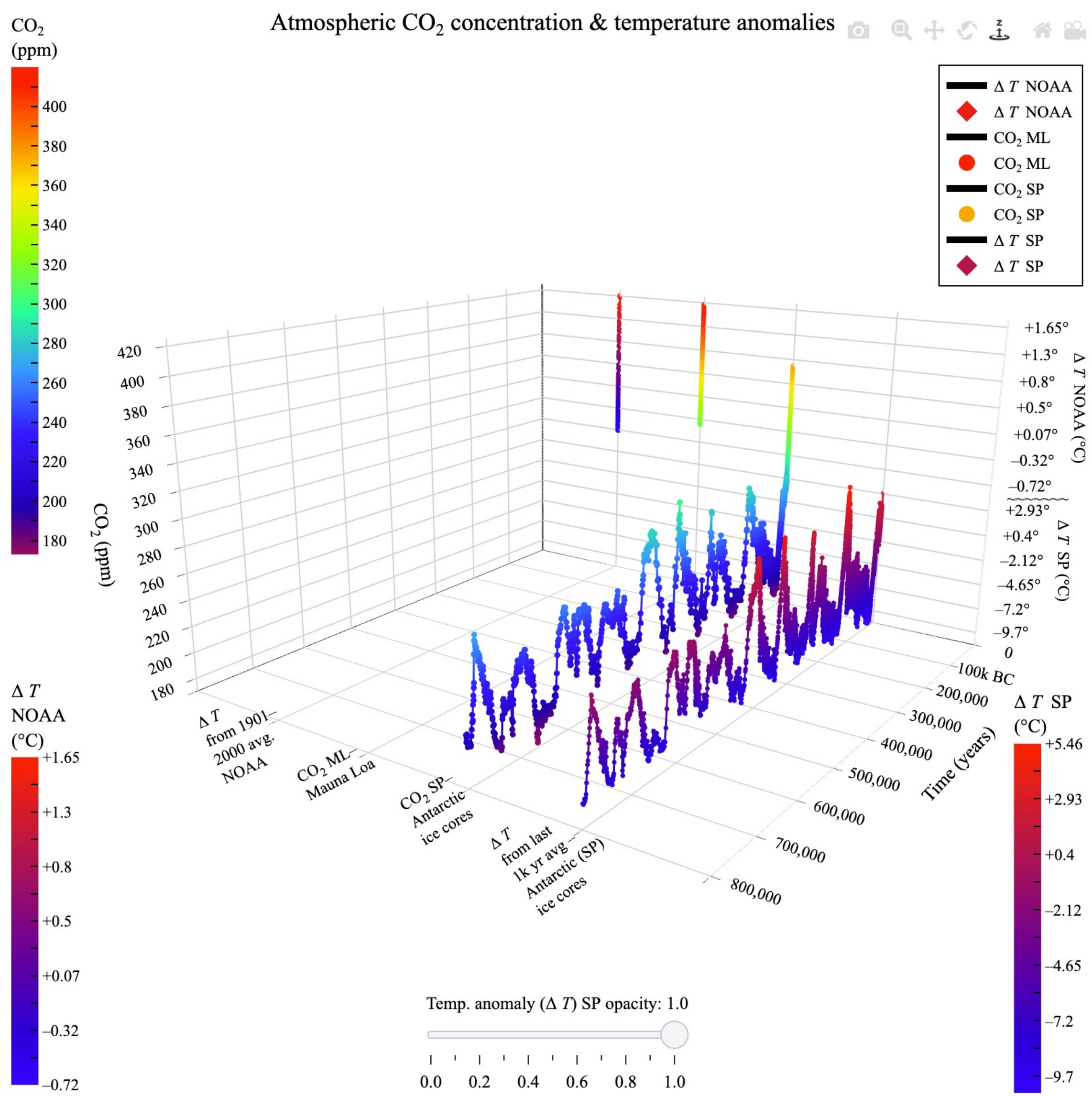

(Noble 2024)

Keeling curve and related datasets

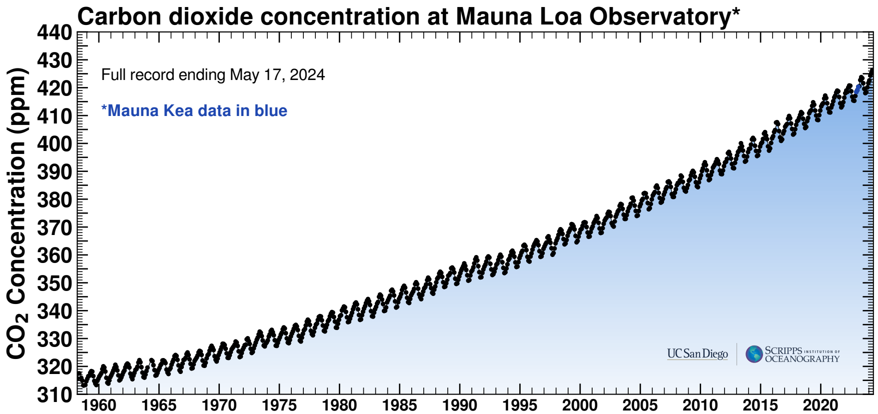

(Keeling 2024)

Figure 5.6 | Time series of CO_2 concentrations and related measurements in ambient air. (a) Concentration time series and MLO-SPO difference, **(b)** growth rates, **(c)** ^{14}C and ^{13}C isotopes, and **(d)** O_2/N_2 ratio. The data for Mauna Loa Observatory (MLO) and South Pole Observatory (SPO) are taken from the Scripps Institution of Oceanography (SIO)/University of California, San Diego (Keeling et al., 2001). The global mean CO_2 are taken from National Oceanic and Atmospheric Administration (NOAA) cooperative network (as in Chapter 2), and Greenhouse Gases Observing Satellite (GOSAT) monthly mean XCO_2 (mixing ratio) time series are taken from National Institute for Environmental Studies (Yoshida et al., 2013). CO_2 growth rates are calculated as the time derivative of deseasonalized time series (Nakazawa et al., 1997). The $D(O_2/N_2)$ are expressed in per meg units (= (FF/M) × 10^6, where FF = moles of O_2 consumed by fossil-fuel burning, M = 3.706 × 10^{19}, total number of O_2 molecules in the atmosphere (Keeling and Manning, 2014). The $^{14}CO_2$ time series at Barring Head, Wellington, New Zealand (BHD) is taken from GNS Science and NIWA (Turnbull et al., 2017). The multivariate ENSO index (MEI) is shown as the shaded background in panel (b); (warmer shade indicates El Niño). Further details on data sources and processing are available in the chapter data table (Table 5.SM.6).

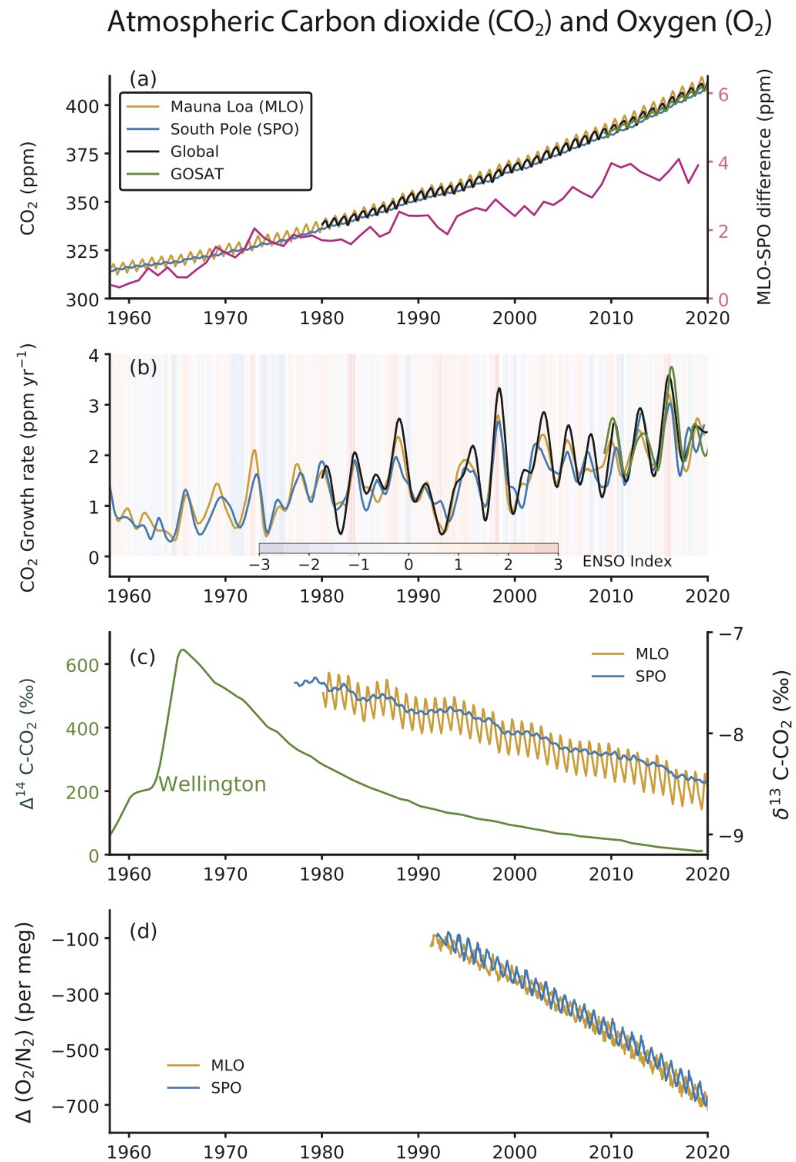

(IPCC 2021)

References

Keeling, C.D., et al., 1976: Atmospheric carbon dioxide variations at Mauna Loa observatory, Hawaii. *Tellus*, **28**, p.6.

Keeling, C.D., 2024: Keeling CO_2 dataset. keelingcurve.ucsd.edu.

IPCC, 2021: Climate Change 2021: The Physical Science Basis. Contribution of Working Group I to the Sixth Assessment Report of the Intergovernmental Panel on Climate Change. Cambridge University Press, 2391 pp.

Noble, J., 2024: Visualization of atmospheric CO_2 datasets (software development). jnoble.org/climate.

Pales, J.C. and Keeling, C.D., 1965: The Concentration of Atmospheric Carbon Dioxide in Hawaii. *Journal of Geophysical Research*, **70**, 6053–76.

Price, S. and Pales, J.C., 1959: The Mauna Loa high-altitude observatory. *Monthly Weather Review*, **87**, 1–14.